



**HAL**  
open science

## Laterally static and cyclic pile behavior in clay

Meriam Khemakhem, N. Chenaf, Josselin Garnier, G. Rault, L. Thorel,  
Christophe Dano

► **To cite this version:**

Meriam Khemakhem, N. Chenaf, Josselin Garnier, G. Rault, L. Thorel, et al.. Laterally static and cyclic pile behavior in clay. 7th International Conference on Physical Modelling in Geotechnics, 2010, Zurich, Switzerland. hal-01008379

**HAL Id: hal-01008379**

**<https://hal.science/hal-01008379>**

Submitted on 3 May 2018

**HAL** is a multi-disciplinary open access archive for the deposit and dissemination of scientific research documents, whether they are published or not. The documents may come from teaching and research institutions in France or abroad, or from public or private research centers.

L'archive ouverte pluridisciplinaire **HAL**, est destinée au dépôt et à la diffusion de documents scientifiques de niveau recherche, publiés ou non, émanant des établissements d'enseignement et de recherche français ou étrangers, des laboratoires publics ou privés.

# Laterally static and cyclic pile behavior in clay

M. Khemakhem, N. Chenaf, J. Garnier, G. Rault, L. Thorel  
*Laboratoire Central des Ponts et Chaussées, Nantes, France*

C. Dano

*Institut de recherche en Génie Civil et Mécanique, Nantes, France*

**ABSTRACT:** While deep foundations have been used extensively in clay to support both monotonic and cyclic lateral loading, significant uncertainties still now exist in predicting the field behaviour of such foundations, especially for the cyclic loading. Cyclic loads result of waves and winds forces on offshore structures or on bridge piers, mooring of boat on quays and variable overloads on many constructions and buildings. Useful data on cyclic loading of piles in sand have already been obtained from centrifuge model tests and the purpose of the present study is to provide new data on the response of piles in clay under lateral static and cyclic loads. The clay is a normally consolidated kaolin whose undrained shear strength increases with depth. Testing equipments and soil model preparation are presented in detail. The program of centrifuge tests is presented. Undrained tests on a rigid and flexible pile models (1/50) are performed. In the first test series, the ultimate static load was estimated. For cyclic loads, the pile top deflection was recorded using displacement transducer installed on the model rigid pile. The effect of the number of cycles on the head displacement was discussed.

## 1 INTRODUCTION

Most of practical interest to the engineer is the knowledge of the deflection and the bending moment resulting on foundations. The bending moment is required in the sizing of the foundation and the deflection is necessary to define the serviceability of the supported structure under static or cyclic loading conditions.

Theoretical approaches including specification about cyclic were developed to predict the behavior of piles in clay: the elastic continuum analysis proposed by Poulos (1982), the non linear subgrade reaction developed by Matlock (1960), the finite elements model of Randolph (1977). These approaches were validated and developed by filed tests carried on full scale-pile (Matlock, 1970 ; Tassios & Leventis, 1974 ; Reese & Welch, 1975 ; Brown and al, 1987) . The results of such tests are relevant but these tests are still expensive and quite difficult to realize. The geotechnical centrifuge offers the possibility to field-test large model scale of piles and different types of soil. However, few tests in centrifuge were conducted to determine the behaviour of piles subjected to static and cyclic loading in clay (Hamilton & al, 1991 ; Kitazume & Miyajima, 1994 ; Ilyas & al, 2004).

The experiments described herein were aimed at predicting the load-deflection relationship of rigid and flexible piles driven on normally consolidated clay, submitted successively to static and cyclic loading. Experimental static responses were compared to computed ones. The calculation was done by the Pilate LCPC software which will be presented later.

## 2 TEST PROCEDURE

All tests were conducted at 50 g on the geotechnical centrifuge in the LCPC in Nantes. The radius of the centrifuge is 5.5 m and its maximum acceleration is up to 200 g.

### 2.1 Model piles

Rigid and flexible model piles were manufactured to simulate at 50 g a prototype steel pile with a diameter of  $B = 0,9\text{ m}$  to a depth of  $D = 16\text{ m}$  below the ground surface. The flexible model pile is made of a tubular aluminium pipe with a thickness of  $1\text{ mm}$  . The rigid model pile is a fully aluminium pipe. Hence, only the stiffness rigidity  $E_p I_p$  differs from

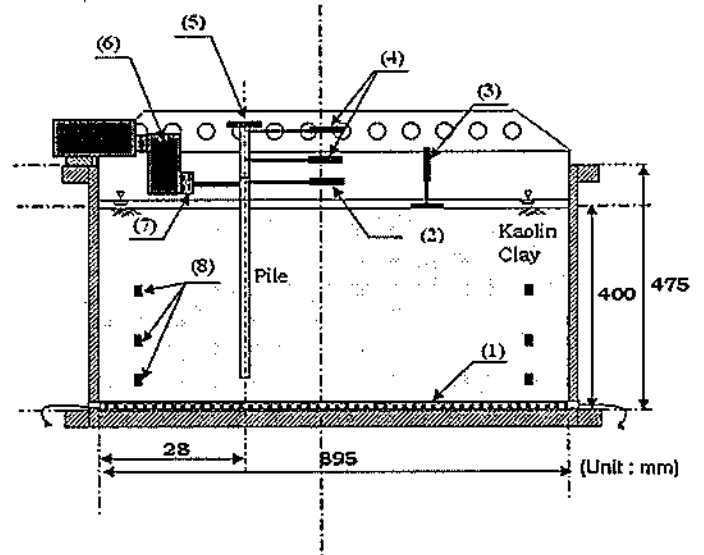
rigid to flexible model pile. The table behind summarize the proprieties of the prototype piles.

Table 1. Proprieties of the prototype piles

	$B$ (m)	$D$ (m)	$E_p I_p$ (MNm <sup>2</sup> )
Flexible pile	0,9	16	895
Rigid pile	0,9	16	38100

The pile instrumentation is presented in the Figure 1. The lateral displacement of the pile head was recorded by a displacement transducer (2) which was mounted in front of the loading point. The pile head was extended so that it was possible to mount two additional displacement transducers (4). This data is important to ensure a redundant measurement. The vertical displacement of the pile is also controlled by a displacement transducer mounted in the head of the pile (5).

A typical model set up for tests is schematically shown in Figure 2. The test layout is also presented in the Figure 3. Lateral loading was applied using in flight a servo-actuator (6) controlled from the centrifuge operator's room. The lateral load was recorded by a load transducer (7) mounted in the servo-actuator. All data were recorded using transducers connected to a microprocessor.



- (1) Drainage geotextile
- (2) Horizontal displacement transducer at the loading point
- (3) Soil settlement transducer
- (4) Horizontal pile displacement transducer
- (5) Vertical pile displacement transducer
- (6) Servo - actuator
- (7) Load transducer
- (8) Pore water transducer

Figure 2. Model set up

## 2.2 Clay sample

### 2.2.1. Preparation - Preliminary consolidation

Tests were performed in a cylindrical steel tubs 895 mm in diameter by 475 mm deep. The kaolin clay named Speswhite and used in this study was homogenous and saturated. The table 2 lists its main physical proprieties.

Table 2. Physical proprieties of kaolin clay

Average bulk unit weight	$\gamma = 17.5 \text{ kN/m}^3$
Final average water content	$w = 50\%$
Compression index	$C_c = 0,44$
Vertical index of consolidation	$C_v = 3 \cdot 10^{-7} \text{ m}^2/\text{s}$
Swelling index	$C_s = 0,44$

Clay sample was prepared in order to reproduce filed conditions at 50 g like in normally consolidated clay. This technique of preparation was used in the LCPC to simulate deep-water anchorages and severals other kinds of offshore plate form foundations (EXXON - CHEVRON).

Three layers were successively poured in the model container. Each layer was prepared and consolidated in the following manner. First, a clay slurry

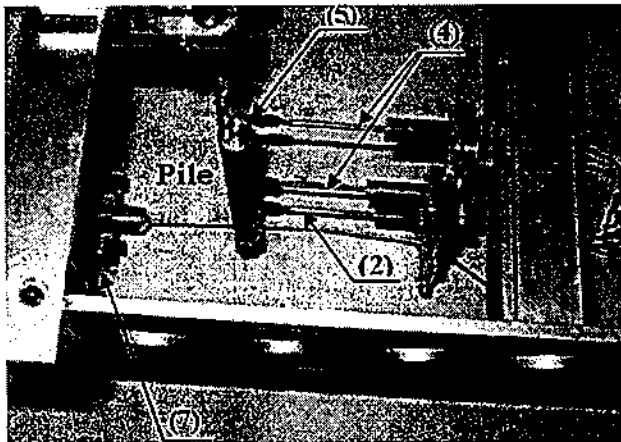


Figure 1. Pile instrumentation

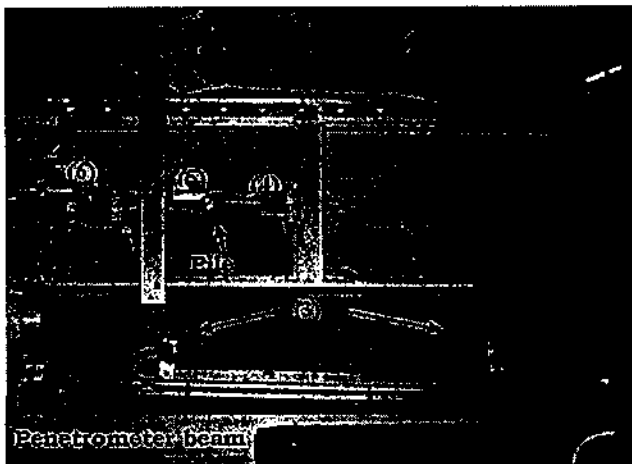


Figure 2. Model test layout

was prepared with an initial average water content  $w = 90\%$  and allowed to rest for 24 hours. Before being placed in the container, the slurry was mixed for about four hours and a drainage geotextil was disposed at its bottom. Second, to reduce the flight time necessary to the final consolidation, this layer was preliminary consolidated at 1g under the value of the overburden pressure enhanced at its center like in 50 g field normally consolidated clay. This pressure is applied by stages. This process was repeated for each layer. When the preliminary consolidation of a layer was achieved, the next layer was placed above and then consolidated. The figure below (Fig.4) presents the theoretical pressure applied for each layer. The preliminary consolidation is followed by the in-flight consolidation. This process ensure the ultimate consolidation of the clay sample

The theoretical final height of each layer after the preliminary consolidation at 1g was about 133 mm., the final model sample thickness was about 400 mm. The pile was installed at 1g by driving it into a drilled hole before turning on the centrifuge.

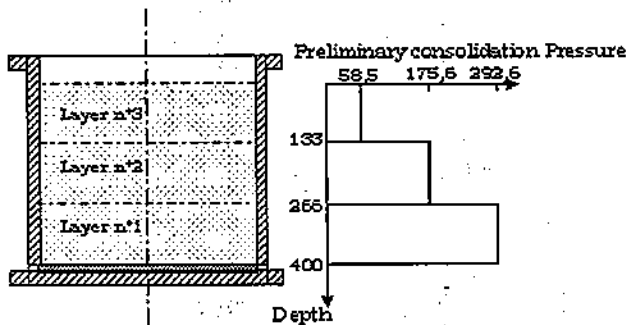


Figure 4. Preliminary consolidation pressure

### 2.2.2. In flight Consolidation

The clay sample was then reconsolidated under its self weight in the centrifuge at 50 g to allow the excess pore water pressure to dissipate through the free surface clay and the opening holes at the bottom. Free water approximately 15 mm deep was maintained above the ground soil to ensure the saturation.

Settlements and pore water transducers were used in order to control the consolidation ratio during the in-flight. Two series of three pore water transducers are placed into the clay through holes distributed in the container's wall. Two settlements transducer were placed above the soil free surface (see Fig.2).

A settlement graphical method was mainly used to estimate and to control the consolidation ratio at any time from the settlement data during the in-flight. This method, simple and practice, was first proposed by Asaoka (1978) and then developed by Magnan and Deroy (1980). First, a time interval  $\Delta t$  was chosen, in this study  $\Delta t = 20 \text{ mn}$ . Then, during the in-flight, the settlement  $s_i$  was measured at the time  $t_i$  as shown in the table below (Tab. 2),  $s_{i-1}$  and

$s_i$  are successively the settlements recorded at two successive time steps  $t_{i-1}$  and  $t_i = t_{i-1} + \Delta t$ . The values of  $s_{i-1}$  are then plotted versus  $s_i$ . The final settlement  $S_\infty$  is the intersection of this curve and the bisector. The final predict settlement and the last measured average settlement give the consolidation ratio:

$$U = \frac{s(t)}{S_\infty} \times 100 (\%) \quad (1)$$

Table 2. Asaoka method

t (mn)	$t_1$	$t_2$	$t_3$	$t_4$	$t_5$	$t_6$	...
s (mm)	$s_1$	$s_2$	$s_3$	$s_4$	$s_5$	$s_6$	...

Generally, a value at least equal to  $U = 70\%$  was achieved before starting the pile loading. The final model sample thickness after the in-flight consolidation was about 395 mm. For each model container, four tests were performed. The consolidation in flight had to be repeated for each test: the centrifuge was stopped to adjust the position of the servo-actuator to conduct the next test. The duration of consolidation was unpredictable. We have noted that the consolidation in the first tests was faster and better than the subsequent ones. If a maximum of four hours was necessary to achieve  $U = 85\%$  for the first and the second tests, the latest required about six hours to reach 71% of consolidation.

### 2.2.3. Penetrometer test

Undrained shear strength of the soil was measured at 1g and in flight after the final consolidation process using a cone penetrometer. The penetrometer used has a cross bar of 300 mm long and 12 mm in diameter attached perpendicularly to the end of a vertical shaft. The cone was pushed in the soil at a rate of 5 mm/s and its penetration resistance  $q_c$  was monitored by a cell load cell fastened onto the cone. The depth of penetration was monitored by a potentiometer located inside the actuator. Undrained shear strength  $S_u$  was then calculated using a correlation between the penetrometer resistance and the scissometer undrained shear strength which was checked in the LCPC for the same normally consolidated clay :

$$q_c = 18,5 S_u \quad (2)$$

## 2.3 Experimental program

In this study, results of five tests will be presented. Static and cyclic lateral load tests were carried out. After the completion of the consolidation in-flight, each pile was laterally loaded at its top.

Static loading tests were performed to estimate the ultimate lateral load of the interaction soil-pile. The load is applied using displacement control mode at a rate of  $4\text{ mm/s}$ . Lateral displacement was applied on pile until the load recorded did not increase and became constant. This rate was chosen so that the conditions around the pile during the loading are essentially undrained. This rate was estimated from T-bar tests performed in a centrifuge at the University of Western Australia by Steward and Randolph (1991). Authors suggested two approximate limits of loading's rates between the drained (Eq. 3) and undrained conditions (Eq. 4). The rate depends on the T-bar diameter  $B$  and the vertical consolidation index  $C_v$ .

$$v < \frac{0,2 C_v}{B} \text{ for drained conditions} \quad (3)$$

$$v > \frac{20 C_v}{B} \text{ for undrained conditions} \quad (4)$$

The limit rate for undrained conditions was estimated for these tests, it was found that

$$v > 3\text{ mm/s}$$

For cyclic loading, a rigid pile was subjected to one-way cyclic loading using loading control mode. The cyclic input was a fifty-cycles sinusoidal sequence with a frequency of  $0,5\text{ Hz}$ . The amplitude was fixed at twenty per cent of the ultimate lateral load estimated in the static tests. A typical record of the load applied is given in Figure 5.

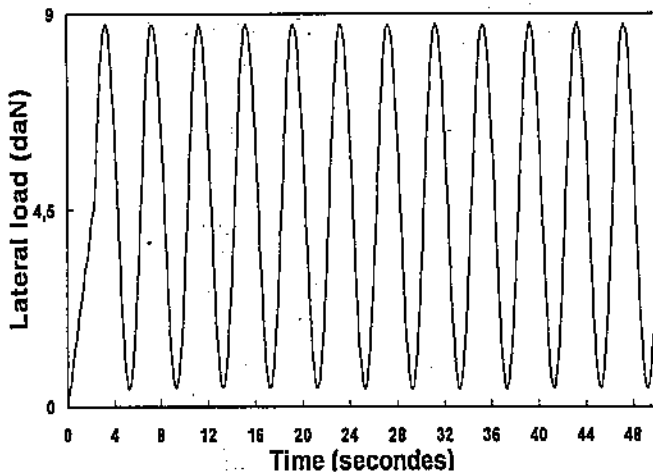


Figure 5. Beginning of cyclic load sequence in model scale

### 3 . TEST RESULTS

All results presented herein are in prototype scale.

#### 3.1 Undrained shear strength profile

Results reveal as expected that the soil strength increase linearly with the depth both at  $1\text{ g}$  and at  $50\text{ g}$

as shown in Fig.6. The consolidation was achieved in flight, thus the values of the undrained shear strength were higher at  $50\text{ g}$ .

As mentioned, the re-consolidation in flight was unavoidable. For each test, a penetrometer test had to be done. The comparisons between the shear strength profile at  $50\text{ g}$ , for all test, show that the soil resistance was almost comparable.

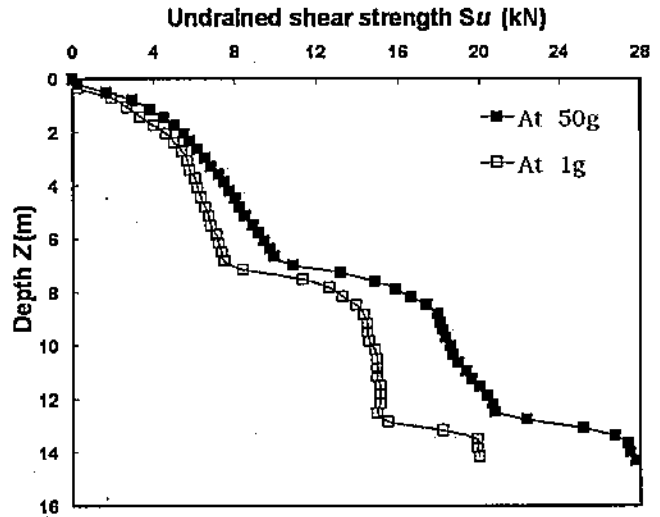


Figure 6. Undrained shear strength profile

#### 3.2 Ultimate lateral static load

##### Load-displacement relationship

After all tests completed, a gap was observed in front of the pile. The soil behind the pile was confined as shown in Fig.7.

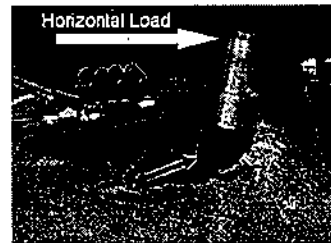


Figure 7. Gap after test completed

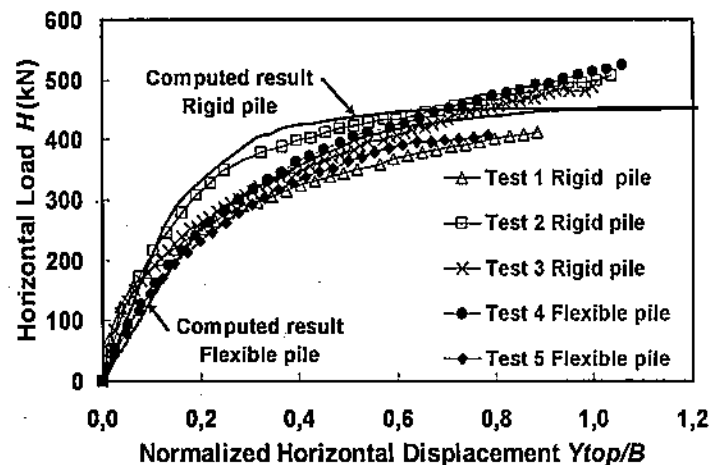


Figure 8. Static lateral load-displacement relationship

The relationship between lateral load and lateral displacement at the loading point is drawn as shown in Fig. 9, the horizontal displacement was normalized with respect to the pile diameter  $B$ . As expected, the applied load increased with applied displacement. For small displacement, the lateral load  $H$  can be considered to increase linearly with the top deflection of the pile  $y_{Top}$ . This relation can be expressed by the following equation:

$$H = k y_{Top} \quad (5)$$

Where  $k$  is a coefficient of the soil-pile interaction. We noted that equal stiffness rigidity piles have approximately the same coefficient  $k$ . In addition, the coefficient  $k$  for rigid piles was higher than flexible ones for all tests. We concluded that the lateral load for small displacements depends on the stiffness rigidity of the pile considered. Centrifuge tests were conducted by Katuzume & Miyajima (1994), it was found that the horizontal load increased almost linearly with the increase of the square root of pile rigidity.

For higher displacement, the results emphasize the highly non linearity nature of the soil- pile- interaction. The ultimate load  $H_u$  was deduced from the load-displacement. A value between 400 and 500 kN was approximately found for all piles regardless the stiffness rigidity.

The lateral load- displacement relationship was also computed using the Pilate LCPC software which is based on the elastic continuum analysis. Calculated P-y curves, stiffness rigidity of piles and boundary conditions were introduced first into Pilate. The pile tip was supposed free. The results obtained for each load increment are presented in Fig. 9. It is a fair agreement with the measured curves. Moreover, it can be seen that the difference still exists between the responses for rigid and flexible piles. The coefficient of the interaction soil-pile of rigid pile remains higher than the flexible one for small displacement. Finally, the ultimate load was the same for the highest displacement as experimental results.

### 3.3 Pile head displacement under cyclic lateral load

The cyclic curve of load-displacement at the loading point is shown in Figure 9. In the first loading stage, before the first cycle, the horizontal displacement rose up to  $y_1$ . After the first cycle, a residual displacement was accumulated with increasing cycles for the same load. The displacement normalized with the displacement  $y_1$  versus the number of cycles is presented in the Figure 10. As shown, the normalized ratio  $y/y_1$  increased with the number of cycles for the same load, but no stabilization was reached.

It is reasonable to attribute this phenomenon to the degradation of clay's strength under cyclic loading, which contribute to increase the displacement. Cyclic simple shear loading tests were carried on clay (Purzin & al, 1995), it was seen that the mean effective stresses decreases and so the clay was no longer as resistant as before cyclic loading. A slight increase of the pore pressure may cause the degradation of the soil.

The last issue to be discussed in this section concerns the comparison between the behavior of the head pile under cyclic loading in the sand (Rosquoët, 2004) and in the clay. We noted a fair agreement between them. The top displacement of the pile embedded in the sand was fitted by a logarithmic curve:

$$\frac{y_n}{y_1} = 1 + b \ln(N) \quad (6)$$

Where  $b$  is a coefficient depending on the amplitude and the density of the soil. and  $N$  is the number of cycles applied.

A similar fitting is possible to piles embedded in clay, but more tests are needed to define parameters which could affect the coefficient  $b$ . These parameters could be the amplitude, the consolidation degree or both.

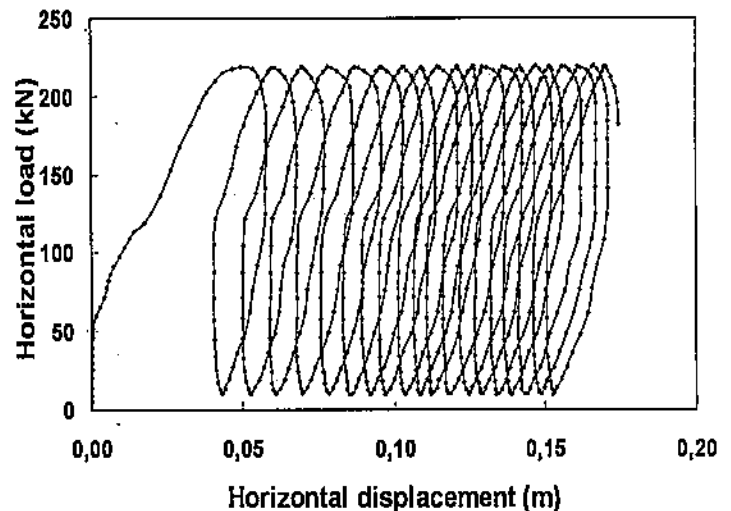


Figure 9. Cyclic lateral load –displacement relationship

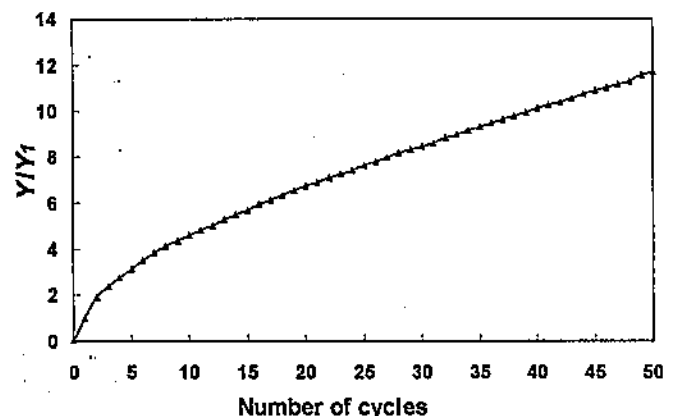


Figure 10. Normalized displacement – number of cycles relationship

## 4 CONCLUSION

The behavior of the pile embedded in normally consolidated clay under static and cyclic lateral loading was undertaken in this study. The displacement of the head pile was investigated. Results were reproducible despite the stopping of the centrifuge and the reconsolidation of the sample clay for each test. Careful supervision was needed to avert the clay's swelling. In fact, it was necessary to aspirate the water above the ground surface as soon as the centrifuge was stopped. In sum, the following conclusions were obtained:

1) The lateral load-displacement relationship depends on the stiffness rigidity of piles. This result was affirmed by calculation (Pilate).

2) The ultimate lateral load deduced from the load-displacement curve at the loading point was reproducible regardless the stiffness rigidity of pile.

2) Cyclic loading could cause the degradation of the normally consolidated clay, thus the pile head displacement didn't reach stabilization.

For a through investigation, tests with more significant number of cycles are needed to define probably a stabilization threshold of the residual displacement. In addition, an accurate measure of the pore pressure nearer to the pile is particularly relevant even if the conditions are supposed undrained according to Steward & Randolph (1991). The purpose of these measurements is to focus on the causes of the degradation of the soil around the pile under cycles. Lastly, it is necessary to test clay with different consolidation degree to compare the effect of cyclic loading on the clay and on the pile head displacement under the same cyclic loading.

## References

- Asaoka A. 1978. Observation procedure of settlement prediction. *Soils and foundations*, Vol. 18, No. 4, 1978. Japanese Society of Soils Mechanics and Foundation Engineering, dec 1978, pp. 87-101
- Brown D.A., Reese L.C. & O'Neill, M.W. 1987. Cyclic lateral loading of a large scale pile groupe. *Journal of Geotechnical Engineering*, 1987, Vol. 113(11), pp. 1326-1343
- G.Poulos, H. 1982. Single pile response to cyclic lateral. *Journal of Geotechnical Engineering Division ASCE*, 1982, Vol. 108(GT), pp. 355-375
- Hamilton, J.M., Dunnivant, T.W & Murff, J.D. 1991. Centrifuge study of laterally loaded behavior in clay. *Centrifuge 1991*, pp. 285-292
- House A.R, Oliveira, J.R.M.S. & Randolph M.F. 2001. Evaluating the coefficient of consolidation using penetration tests. *International Journal of Physical Modelling in Geotechnics* 3 (2001), pp. 17-26

Ilyas, T., Leung, C.F., Chow, Y.K. & Budi, S.S. 2004. Centrifuge model study of laterally loaded pile groups in clay. *Journal of Geotechnical and Geoenvironmental engineering*, 2004, Vol. 130(3), pp. 274-283

Kitazume, M. & Miyajima, S. 1994. Lateral resistance of a long pile in soft clay. *Centrifuge 1994*, pp. 485-490

Magnan JP & Deroy JM. 1980. Analyse graphique des courbes de consolidation oedométrique. *Bulletin de Liaison des Ponts et Chaussées*, sep-oct. 1980, pp. 53-56

Magnan JP & Deroy JM. 1980. Analyse graphique des tassements observés sous les ouvrages. *Bulletin de Liaison des Ponts et Chaussées*, sep-oct. 1980, pp. 45-52

Reese, L & Welch, R. 1975. Lateral loading of deep foundations in stiff clay. *Journal of geotechnical engineering division, Proceedings of the American Society of Civil Engineering*, Vol. 101, No. GT7, July, 1975, pp. 633-649

Rosquoët, F. 2004. Pieux sous charge latérale cyclique. Thèse de Doctorat, Ecole Centrale de Nantes, Université de Nantes, France, 305p. (in French).

Purzin A, Frydman S & Talesnick, M. 1995. Normalized non-degrading behavior of soft clay under cyclic simple shear loading. *Journal of Geotechnical Engineering*, 1995, Vol. 121(12), pp. 836-843

Tassios, T & E. Levendis E. 1974. Efforts répétitifs horizontaux sur pieux verticaux. *Annales de l'institut technique du bâtiment et des travaux publics*. No. 315, 1974, pp. 45-71